

1  
2  
3  
4  
5  
6  
7  
8  
9  
10  
11  
12  
13  
14  
15  
16  
17  
18  
19  
20  
21  
22  
23  
24  
25  
26  
27  
28  
29  
30  
31  
32  
33  
34  
35  
36  
37  
38  
39  
40  
41  
42  
43  
44  
45  
46  
47  
48  
49  
50  
51  
52  
53  
54  
55  
56  
57  
58  
59  
60  
61  
62  
63  
64  
65

Research News

Modulating flow topology in microdroplets to control reaction kinetics

Shaohua Ma<sup>1,2,\*</sup>, Haoran Zhao<sup>1,2</sup>, Edgar A. Galan<sup>1,2</sup>, Stavroula Balabani<sup>3</sup>

<sup>1</sup>Institute of Biopharmaceutical and Health Engineering (iBHE), Shenzhen International Graduate School (SIGS), Tsinghua University, Shenzhen, 518055, China.

<sup>2</sup>Tsinghua-Berkeley Shenzhen Institute (TBSI), Tsinghua University, Shenzhen, 518055, China.

<sup>3</sup>Department of Mechanical Engineering, University College London, London WC1E 6BT, UK

\*Email: ma.shaohua@sz.tsinghua.edu.cn

1  
2  
3  
4 **Abstract**  
5  
6

7 In traditional reaction flasks, the reaction rate of macromolecular compounds is dictated by the  
8 concentrations and distribution of reactants along with their intrinsic reaction kinetics. **Controlling reaction**  
9 **kinetics** in microfluidic droplets has been proposed through the regulation of flow dynamics, but is yet to  
10 be demonstrated experimentally. Here, we verify this hypothesis by accelerating or suppressing  
11 macromolecular **reactant mixing** in microfluidic droplets. The control of reaction kinetics through the  
12 modulation of flow topology in microdroplets might enable further developments in modelling  
13 macromolecular systems.  
14  
15  
16  
17  
18  
19  
20  
21  
22  
23  
24  
25  
26  
27  
28  
29  
30  
31  
32  
33  
34  
35  
36  
37  
38  
39  
40  
41  
42  
43  
44  
45  
46  
47  
48  
49  
50  
51  
52  
53  
54  
55  
56  
57  
58  
59  
60  
61  
62  
63  
64  
65

1  
2  
3  
4 The emergence of microfluidics and lab-on-a-chip technologies enabled the miniaturization of experimental  
5  
6 laboratory procedures onto penny-sized chips. These chips are composed of networks of microchannels and  
7  
8 reservoirs, which are analogous to beakers and pipettes in a standard chemistry laboratory. Droplet-based  
9  
10 microfluidics allows parallel reactions to take place in compartmentalized droplets with high throughput,<sup>1-</sup>  
11  
12 <sup>3</sup> which is accomplished by downsizing the reaction volumes by several of magnitude into thousands of  
13  
14 identical microdroplets.<sup>4-6</sup> Additionally, droplet reactors help reduce cross contamination as the reactants  
15  
16 are usually confined by the interface formed between the droplet surface and an immiscible continuous  
17  
18 phase.  
19  
20

21  
22 Numerous experimental and simulation studies have shown the high efficiency that comes with mixing  
23  
24 within microdroplets, which is attributed to the unique molecular transport mechanisms occurring at the  
25  
26 microscale and the internal flow dynamics generated by the droplet movement.<sup>7-9</sup> This aspect of flow  
27  
28 dynamics can be modulated, enabling the precise control of reaction mixing and timings.<sup>10</sup> In a straight  
29  
30 microchannel, the fluid within a droplet tends to form two symmetrical hemispheres with continuous flow  
31  
32 recirculation divided by a stable interface in the middle. This topology suppresses convection in the  
33  
34 direction perpendicular to the flow, which enables the production of Janus particles by independently  
35  
36 crosslinking dissimilar polymers contained in each hemisphere.<sup>11</sup> Meanwhile, microchannels featuring  
37  
38 curves induce convective mixing in droplets, facilitating the generation of particles with homogeneous  
39  
40 compositions.<sup>12-14</sup> Additionally, droplets containing phase-separated liquids are useful to generate  
41  
42 anisotropic microstructures.<sup>15,16</sup>  
43  
44  
45  
46  
47

48 The manipulation of droplet flow topology can be applied in more complex scenarios. For example, the  
49  
50 droplet's internal circulation can be increased or suppressed to achieve higher or reduced shear forces and  
51  
52 mixing efficiencies. The flow topology is regulated by several physical parameters, including the capillary  
53  
54 and Reynolds numbers, surface tension, Marangoni effects, and droplet morphology, with viscosity playing  
55  
56 a dominant role over the others.<sup>17-19</sup> Apart from intrinsic reaction kinetics, the rates of chemical and  
57  
58 biological reactions are correlated with the local concentration and transport efficiency of reactants. With  
59  
60  
61  
62  
63  
64  
65

1  
2  
3  
4 this in mind, rapid mixing in microdroplets has been proposed to improve the mixing performance in a sol-  
5 gel transition,<sup>9</sup> as well as allowing for more efficient chemical and biological reactions.<sup>20</sup> However,  
6  
7 controlling reactions through the regulation of droplet flow topology has not been extensively studied  
8  
9 experimentally.

10  
11  
12  
13  
14 We have previously used centroid location-based ensemble correlation to reduce the noise in velocity  
15  
16 vectors obtained from microparticle image velocimetry ( $\mu$ PIV) to investigate the three-dimensional flow  
17  
18 topology in two different types of droplets. The flows were characterized by distinct circulation and shear  
19  
20 profiles, which were observed to be mainly regulated by the viscosity ratios across the interfaces of droplets.  
21  
22 The average flow within the droplet in reference to the droplet itself increases along with the inner-to-outer  
23  
24 phase viscosity ratio  $\lambda$ . This work demonstrates that chemical reactions can be controlled by varying the  
25  
26 viscosity of the continuous phase.  
27  
28  
29

30  
31 The two types of droplets ( $\lambda = 0.12$  and  $\lambda = 0.78$ ) studied by Ma et al.<sup>17,18</sup> exhibit distinctive flow  
32  
33 topologies. One droplet ( $\lambda = 0.12$ ) features a relatively high volumetric internal flow regardless of its size  
34  
35 (Figures 1 and 2a), whereas the other droplet ( $\lambda = 0.78$ ) presents a small internal flow, except for symmetric  
36  
37 recursive flows along the droplet boundaries (Figure 2b).

38  
39  
40 Figure 1 shows the axial and transverse flow profiles in droplets of various sizes when  $\lambda = 0.12$ . The flow  
41  
42 topology remains unchanged independently of the droplet morphology, and the dominant velocities are the  
43  
44 axial in the center and the transverse in the diagonal corners. However, the droplet morphology does affect  
45  
46 the flow magnitude, i.e., larger droplets have a larger contact area with the channel walls, which results in  
47  
48 increased friction and enhances internal flow circulation.  
49

50  
51  
52 Figure 2 shows the droplet flow topology at different cross-sectional planes and velocities (axial  $U$  and  
53  
54 transverse  $V$ ). Since gravity has negligible effects in microfluidic systems<sup>16</sup> and the boundary conditions  
55  
56 are constant along the interface, it can be assumed that the flow topologies in the mid-xz and mid-yz planes  
57  
58 are identical to the topology in the mid-xy plane. The flow topology is totally different for the two droplets  
59  
60  
61  
62  
63  
64  
65

( $\lambda = 0.12$  and  $\lambda = 0.78$ ) in Figure 2. For example, the  $\lambda = 0.78$  droplet is composed of fluids with significantly reduced axial and transverse velocities in the bulk volume, thus the positive axial flow observed on the lower planes are possibly a result of the gutter flow between the water-oil interface and the rectangular channel boundaries.<sup>21</sup>

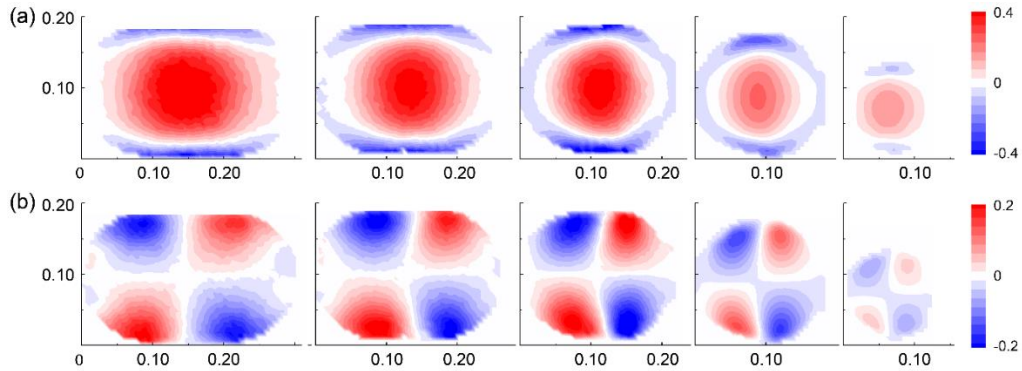
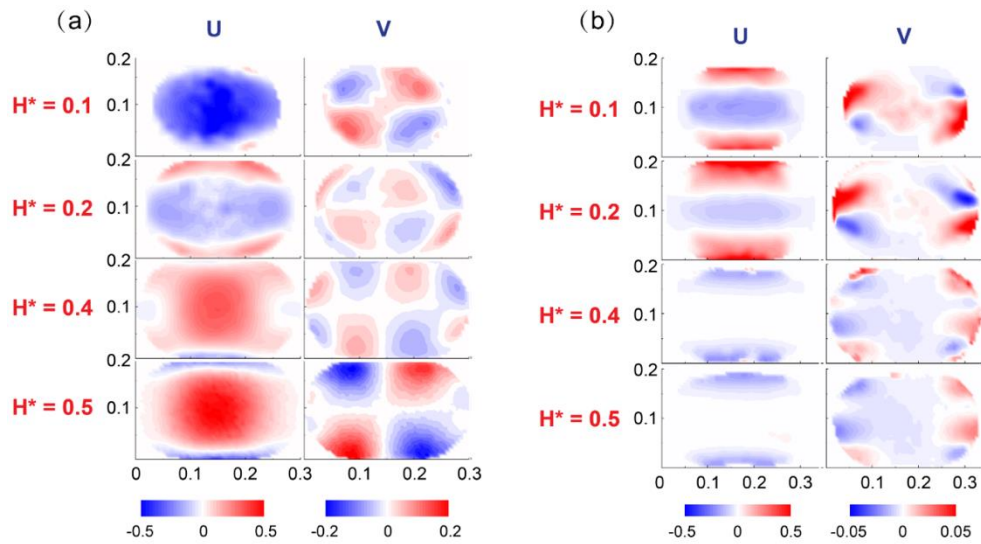


**Figure 1.** Cross-sectional view of flow topologies at the center of droplets of various sizes flowing through a rectangular microchannel when  $\lambda = 0.12$ , showing the (a) axial and (b) transverse velocities  $U$  and  $V$ , respectively. Both components are normalized to the droplet velocity  $v_d$  (i.e.,  $U = u/v_d$  and  $V = v/v_d$ ).

The axial and transverse velocities are positive when the velocity component points in the direction normal or perpendicular (pointing down) to the flow, respectively.



1  
2  
3  
4 **Figure 2.** Visualization of  $U$  and  $V$  at four cross-sectional focal planes in droplets of the same size, when  
5  
6 (a)  $\lambda = 0.12$  and (b)  $\lambda = 0.78$ .  $H^*$  represents the position of the focal plane in relation to the height of the  
7  
8 droplet, where  $H^* = 0.5$  represents the focal plane across the middle of the droplet. The axial and transverse  
9  
10 velocities are positive when the velocity component points in the direction normal or perpendicular  
11  
12 (pointing down) to the flow, respectively.  
13  
14  
15

16 It has been shown that the mixing efficiency is directly related to the magnitude of the flow components  $U$   
17  
18 and  $V$ .<sup>9</sup> Therefore, it must be possible to control the mixing efficiency of chemical reactions by modulating  
19  
20 the viscosity ratio across the droplet interface. To our knowledge, the control of reaction kinetics through  
21  
22 the modulation of flow topology has not been demonstrated experimentally. In a static microdroplet,  
23  
24 molecular diffusion acts as the only mass transport mechanism. Therefore, to evaluate mixing performance  
25  
26 as modulated via flow topology, one must use a system with negligible passive mixing (diffusion), so that  
27  
28 the droplet internal flow circulation acts as the sole mixing mechanism. Recently, ultra-long single-strand  
29  
30 DNA and its complementary sequence has been employed to control the crosslinking of collagen.<sup>22</sup> The  
31  
32 reaction remains suppressed in static conditions and is only initiated when the mixture starts flowing  
33  
34 through a microfluidic channel. The crosslinking occurs when the nucleic acid bases on the DNA form  
35  
36 electrostatic bonds with the complementary sequence (Figures 3a and 3b).  
37  
38  
39  
40

41 The internal flow circulation in droplets is regulated by  $\lambda$  (Figure 2). At higher  $\lambda$ , with HFE7000 (3M, US)<sup>23</sup>  
42  
43 as the continuous phase, the internal circulation is reduced and the internal flow velocity becomes uniform.  
44  
45 Crosslinking is restricted, resulting in a lack of gelation in the droplets (Figure 3c). Using HFE7500 (3M,  
46  
47 US)<sup>24</sup> reduces  $\lambda$  over 2 orders of magnitude, greatly improving droplet gelation (Figures 3d and 3e). The  
48  
49 reaction speed takes place about 30 times faster than in native collagen, with gelation times as short as 40  
50  
51 seconds at room temperature.  
52  
53  
54  
55  
56  
57  
58  
59  
60  
61  
62  
63  
64  
65

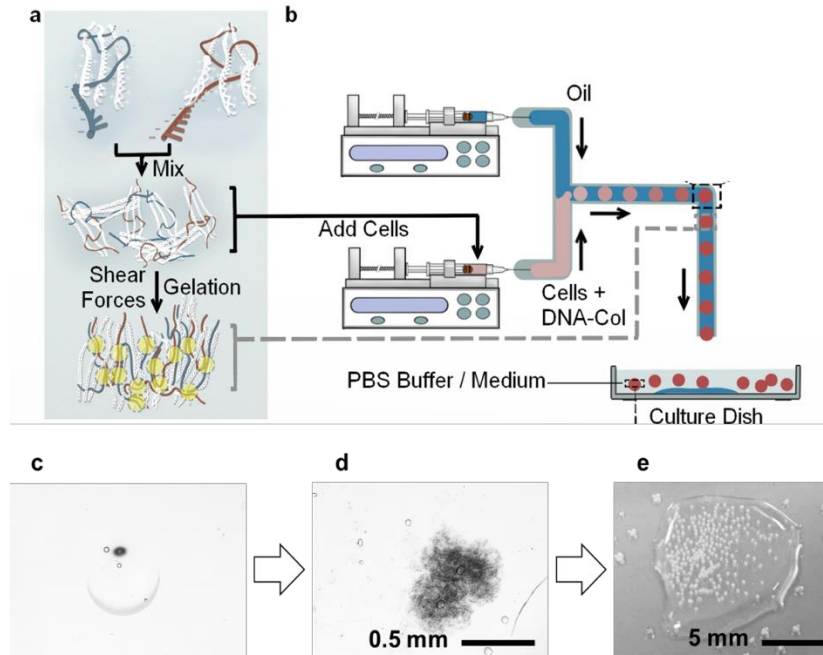


**Figure 3.** Ultra-long single-strand DNA (ssDNA) was used as the crosslinking agent for collagen fibrils. (a) Mixing of ssDNA with its complementary sequence is suppressed in static conditions and only initiated when the mixture is set to flow. (b) Mixing efficiency increases with flow magnitude in microfluidic droplets, which can be controlled through the modulation of  $\lambda$  by varying the viscosity of the continuous phase. The modulation of crosslinking efficiency can be evidenced by the scenarios where (c) the collagen mixture fails to gelate, (d) accomplishes gelation, and (e) achieves homogeneous shapes. The samples were obtained by circulating collagen droplets through a microfluidic channel for 5 minutes at a rate of  $1 \text{ m min}^{-1}$  using (c) HFE7000 and (d and e) HFE7500 as the continuous phase.

We demonstrated the control of reaction kinetics through the modulation of flow dynamics in microdroplets as proof-of-concept experiment. This mechanism is yet to be demonstrated in a pragmatic scenario. It is noted that the proposed method is most efficient in macromolecular reactions where diffusion is negligible, since diffusion as a mixing mechanism is intrinsically efficient in small volumes. We believe that the modulation of flow topology could be useful to probe intracellular activities (e.g., transcription or signal transduction) in living cells, although their composition is much more complex than the homogeneous

1  
2  
3  
4  
5  
6  
7  
8  
9  
10  
11  
12  
13  
14  
15  
16  
17  
18  
19  
20  
21  
22  
23  
24  
25  
26  
27  
28  
29  
30  
31  
32  
33  
34  
35  
36  
37  
38  
39  
40  
41  
42  
43  
44  
45  
46  
47  
48  
49  
50  
51  
52  
53  
54  
55  
56  
57  
58  
59  
60  
61  
62  
63  
64  
65

droplets used here. Future work could focus on developing more complex droplet models that could translate to modelling the contents of cells (e.g., different organelles and cytoskeleton compartments). Additionally, the further exploration of this method might open up new routes to modulate in vitro macromolecular reactions such as the synthesis of antibodies. This could contribute to design efficient biomimetic microreactors. And, although not guaranteed, it is possible that new types of reactions can be designed based on the control of reaction kinetics as demonstrated here.



1  
2  
3  
4 **Acknowledgment**  
5

6  
7 The work was supported by the national natural science foundation of China (Grant Number: 61971255)  
8  
9 and Shenzhen Science and Technology Innovation Committee (Grant Number:  
10  
11 KQJSCX20180327143623167 and KCXFZ202002011010508).  
12  
13  
14  
15  
16  
17  
18  
19  
20  
21  
22  
23  
24  
25  
26  
27  
28  
29  
30  
31  
32  
33  
34  
35  
36  
37  
38  
39  
40  
41  
42  
43  
44  
45  
46  
47  
48  
49  
50  
51  
52  
53  
54  
55  
56  
57  
58  
59  
60  
61  
62  
63  
64  
65

1  
2  
3  
4 **Reference**  
5  
6

- 7 1 P. B. Umbanhowar, V. Prasad and D. A. Weitz, *Langmuir*, 2000, 16, 347–351.  
8  
9  
10 2 T. Thorsen, R. W. Roberts, F. H. Arnold and S. R. Quake, *Phys. Rev. Lett.*, 2001, 86, 4163–4166.  
11  
12  
13 3 S. L. Anna, N. Bontoux and H. A. Stone, *Appl. Phys. Lett.*, 2003, 82, 364–366.  
14  
15  
16 4 A. B. Theberge, F. Courtois, Y. Schaerli, M. Fischlechner, C. Abell, F. Hollfelder and W. T. S.  
17 Huck, *Angew. Chemie - Int. Ed.*, 2010, 49, 5846–5868.  
18  
19  
20  
21 5 S.-Y. Teh, R. Lin, L.-H. Hung and A. P. Lee, *Lab Chip*, 2008, 8, 198.  
22  
23  
24 6 R. Dangla, S. C. Kayi and C. N. Baroud, *Proc. Natl. Acad. Sci.*, 2013, 110, 853–858.  
25  
26  
27 7 G. M. Whitesides, *Nature*, 2006, 442, 368–373.  
28  
29  
30 8 Andrew J. deMello, *Nature*, 2006, 442, 394–402.  
31  
32  
33 9 S. Zhao, A. Riaud, G. Luo, Y. Jin and Y. Cheng, *Chem. Eng. Sci.*, 2015, 131, 118–128.  
34  
35  
36 10 H. Song, D. L. Chen, R. F. Ismagilov, *Angew. Chemie - Int. Ed.*, 2006, 45, 7336–7356.  
37  
38  
39 11 Z. Nie, S. Xu, M. Seo, P. C. Lewis and E. Kumacheva, *J. Am. Chem. Soc.*, 2005, 127, 8058–8063.  
40  
41  
42 12 S. Xu, Z. Nie, M. Seo, P. Lewis, E. Kumacheva, H. A. Stone, P. Garstecki, D. B. Weibel, I. Gitlin  
43 and G. M. Whitesides, *Angew. Chemie - Int. Ed.*, 2005, 44, 724–728.  
44  
45  
46 13 S. Ma, M. Natoli, X. Liu, M. P. Neubauer, F. M. Watt, A. Fery and W. T. S. Huck, *J. Mater. Chem.*  
47 *B*, 2013, 1, 5128–5136.  
48  
49  
50  
51  
52 14 Y. T. Matsunaga, Y. Morimoto and S. Takeuchi, *Adv. Mater.*, 2011, 23, 90–94.  
53  
54  
55 15 S. Ma, J. Thiele, X. Liu, Y. Bai, C. Abell and W. T. S. Huck, *Small*, 2012, 15, 2356–2360.  
56  
57  
58 16 J. Thiele, V. Chokkalingam, S. Ma, D. A. Wilson and W. T. S. Huck, *Mater. Horizons*, ,  
59 DOI:10.1039/c3mh00043e.  
60  
61  
62  
63  
64  
65

1  
2  
3  
4  
5  
6  
7  
8  
9  
10  
11  
12  
13  
14  
15  
16  
17  
18  
19  
20  
21  
22  
23  
24  
25  
26  
27  
28  
29  
30  
31  
32  
33  
34  
35  
36  
37  
38  
39  
40  
41  
42  
43  
44  
45  
46  
47  
48  
49  
50  
51  
52  
53  
54  
55  
56  
57  
58  
59  
60  
61  
62  
63  
64  
65

17 S. Ma, J. M. Sherwood, W. T. S. Huck and S. Balabani, *Lab Chip*, 2014, 14, 3611.

18 S. Ma, J. M. Sherwood, W. T. S. Huck and S. Balabani, *Lab Chip*, 2015, 15, 2327–2334.

19 H. Kinoshita, S. Kaneda, T. Fujii and M. Oshima, *Lab Chip*, 2007, 7, 338–346.

20 Y. Xu, J. Lee, Z. Li, T. Ordog, R. C. Bailey and L. Wang, *Lab Chip*, 2018, 18, 2583–2592.

21 V. Van Steijn, C. R. Kleijn and M. T. Kreutzer, *Phys. Rev. Lett.*, 2009, 103, 214501.

22 H. Zhao, Z. Wang, S. Jiang, J. Wang, Z. Hu, P. E. Lobie, S. Ma, Microfluidics synthesis of injectable angiogenic microgels. *Cell Rep. Phys. Sci.* 2020, 1, 100047.

23 HFE7000, 3M: <https://multimedia.3m.com/mws/media/121372O/3m-novec-7000-engineered-fluid-tds.pdf>

24 HFE7500, 3M: <http://multimedia.3m.com/mws/media/65496O/3m-novec-7500-engineered-fluid.pdf>



Click here to access/download  
**Production Data**  
figures.doc

